

Spin polarized parametric pumping

Wu Junling, Baigeng Wang, and Jian Wang^{a)}

Department of Physics, The University of Hong Kong, Pokfulam Road, Hong Kong, China

We have developed a general theory for a parametric pump consisting of a nonmagnetic system with two ferromagnetic leads whose magnetic moments orient at an angle θ with respect to each other. In this theory, the leads can maintain at different chemical potential. As a result, the current is driven due to both the external bias and the pumping potentials. When both θ and external bias are zero, our theory recovers the known theory. In particular, two cases are considered: (a). in the adiabatic regime, we have derived the pumped current for arbitrary pumping amplitude and external bias. (b). at finite frequency, the system is away from equilibrium, we have derived the pumped current up to quadratic order in pumping amplitude. Numerical results show interesting spin valve effects for pumped current.

73.23.Ad, 73.40.Gk, 73.40.-c, 72.10.Bg

I. INTRODUCTION

Recently, there is considerable interest in the parametric pumping¹⁻²⁸. The parametric pump is facilitated by cyclic variations of pumping potentials inside the scattering system and has been realized experimentally by Switkes et al³. On theoretical side, much progress has been made towards understanding of various features related to the parametric pump. This includes quantization of pumped charge^{2,9,20,25}, the influence of discrete spatial symmetries and magnetic field^{5,7}, the rectification of displacement current¹⁰, as well as the inelastic scattering¹¹ to the pumped current. The concept of optimal pump has been proposed with the lower bound for the dissipation derived¹². Within the formalism of time-dependent scattering matrix theory, the heat current and shot noise in the pumping process^{17,23,24,27} has also been discussed. Recently, the original adiabatic pumping theory has been extended to account for the effect due to finite frequency^{14,19}, Andreev reflection in the presence of superconducting lead^{13,28}, and strong electron interaction in the Kondo regime²⁶. This gives us more physical insight of parametric pumping. For instance, the experimental observed anomaly of pumped current at $\phi = 0$ and $\phi = \pi$ can be explained using finite frequency theory¹⁹ as due to the quantum interference of different photon assisted processes. When superconducting lead is present, the interference between the direct reflection and multiple Andreev reflection gives rise to an enhancement of pumped current which is four times of that of normal system¹³. It will be interesting to further extend the parametric theory to the case where the ferromagnetic leads are present. With the theory extended, many

new physics are foreseen²⁹ which may lead to new operational paradigms for future spintronic devices³⁰. In this paper, we have developed a parametric pumping theory for a nonmagnetic system with two ferromagnetic leads whose magnetic moments orient at an angle θ with respect to each other. Our theory is based on nonequilibrium Green's function approach and focused on current perpendicular to plane geometry. Parametric pump generates current at zero external bias. It would be interesting to see the interplay of the role played by pumping potential and external bias if the leads are maintain at different chemical potential²². Hence in our theory, the external bias is also included. In the adiabatic regime, the pumped current is proportional to pumping frequency. In this regime, we have derived the parametric pumping theory for finite pumping amplitude. At the finite pumping frequency, the system is away from equilibrium, we have performed perturbation up to the second order in pumping amplitude and obtained the pumped current at finite frequencies. The newly developed theory allows us to study the pumped current for a variety of parameters, such as the pumping amplitude, pumping frequency, phase difference between two pumping potentials, the angular dependence between the magnetization of two leads, as well as the external bias. We have applied our theory to a tunneling magnetoresistance (TMR) junction³¹. Due to the reported room temperature operation of TMR, the fundamental principle and transport properties of TMR devices has attracted increasingly attention³². Our numerical results show interesting spin valve effect for pumped current. The paper is organized as follows. In section II, we derive the general theory of a parametric pump in the presence of ferromagnetic leads. The numerical results and summary are presented in section III.

II. GENERAL THEORY

The system we examine consists of a nonmagnetic system connected by two ferromagnetic electrodes to the reservoir. The magnetic moment \mathbf{M} of the left electrode is pointing to the z -direction, the electric current is flowing in the y -direction, while the moment of the right electrode is at an angle θ to the z -axis in the $x - z$ plane. The Hamiltonian of the system is of the following form

$$H = H_L + H_R + H_0 + V_p + H_T \quad (1)$$

where H_L and H_R describe the left and right electrodes

$$H_L = \sum_{k\sigma} (\epsilon_{kL} + \sigma M) c_{kL\sigma}^\dagger c_{kL\sigma} \quad (2)$$

$$H_R = \sum_{k\sigma} [(\epsilon_{kR} + \sigma M \cos \theta) c_{kR\sigma}^\dagger c_{kR\sigma} + \sum_{k\sigma} M \sin \theta [c_{kR\sigma}^\dagger c_{kR\bar{\sigma}}] \quad . \quad (3)$$

In Eq. (1), H_0 describes the nonmagnetic (NM) scattering region,

$$H_0 = \sum_{n\sigma} \epsilon_n d_{n\sigma}^\dagger d_{n\sigma} \quad . \quad (4)$$

V_p is the time-dependent pumping potential and H_T describes the coupling between electrodes and the NM scattering region with hopping matrix $T_{k\alpha n}$. To simplify the analysis, we assume the hopping matrix to be independent of spin index, hence

$$H_T = \sum_{k\alpha n\sigma} [T_{k\alpha n} c_{k\alpha\sigma}^\dagger d_{n\sigma} + c.c.] \quad . \quad (5)$$

In these expressions $\epsilon_{k\alpha} = \epsilon_k^0 + qV_\alpha$ with $\alpha = L, R$; $c_{k\alpha\sigma}^\dagger$ (with $\sigma = \uparrow, \downarrow$ or ± 1 and $\bar{\sigma} = -\sigma$) is the creation operator of electrons with spin index σ inside the α -electrode. Similarly $d_{n\sigma}^\dagger$ is the creation operator of electrons with spin σ at energy level n for the NM scattering region. In writing down Eqs.(2) and (3), we have made a simplification that the value of molecular field M is the same for the two electrodes, thus the spin-valve effect is obtained³¹ by varying the angle θ . Essentially, M mimics the difference of density of states (DOS) between spin up and down electrons³¹ in the electrodes. In this paper, we only consider the single electron behavior. The charge quantization is not considered so that our system is not in the Coulomb blockade regime. In addition, for the nonmagnetic regions we are interested in, the Kondo effect can be neglected.

To proceed, we first apply the following Bogliubov transformation³³ to diagonalize the Hamiltonian of the right electrode³⁴,

$$c_{kR\sigma} \rightarrow \cos(\theta/2) C_{kR\sigma} - \sigma \sin(\theta/2) C_{kR\bar{\sigma}} \quad (6)$$

$$c_{kR\sigma}^\dagger \rightarrow \cos(\theta/2) C_{kR\sigma}^\dagger - \sigma \sin(\theta/2) C_{kR\bar{\sigma}}^\dagger \quad (7)$$

from which we obtain the effective Hamiltonian

$$H_\alpha = \sum_{k\sigma} [(\epsilon_{k\alpha} + \sigma M) C_{k\alpha\sigma}^\dagger C_{k\alpha\sigma} \quad (8)$$

$$H_T = \sum_{kn\sigma} [T_{kLn} C_{kL\sigma}^\dagger d_{n\sigma} + T_{kRn} (\cos \frac{\theta}{2} C_{kR\sigma}^\dagger - \sigma \sin \frac{\theta}{2} C_{kR\bar{\sigma}}^\dagger) d_{n\sigma} + c.c.] \quad . \quad (9)$$

In the following subsections, we will consider two cases: (1). parametric pumping in the low frequency limit with finite pumping amplitude. (2). pumping in the weak pumping limit with finite pumping frequency.

A. Pumping in the low frequency limit

In the subsection, we examine the pumping current at low frequency limit while maintaining pumping amplitude finite. In this limit, the system is nearly in equilibrium and we will use the equilibrium Green's function^{35–37} to characterize the pumping process. Using the distribution function, the total charge in the system during the pumping is given by

$$Q(x, t) = -iq \int (dE/2\pi) (\mathbf{G}^<(E, \{V(t)\}))_{xx} \quad (10)$$

where $\mathbf{G}^<$ is the lesser Green's function in real space, x labels the position, and $\{V(t)\}$ describes a set of external parameters which facilitates the pumping process. Within Hartree approximation, $\mathbf{G}^<$ is related to the retarded and advanced Green's functions \mathbf{G}^r and \mathbf{G}^a ,

$$\mathbf{G}^<(E, \{V\}) = \mathbf{G}^r(E, \{V\}) i \sum_\alpha \mathbf{\Gamma}_\alpha f_\alpha(E) \mathbf{G}^a(E, \{V\}) \quad . \quad (11)$$

where $f_\alpha(E) = f(E - qV_\alpha)$. In the low frequency limit, the retarded Green's function in real space is given by

$$\mathbf{G}^r(E, \{X\}) = \frac{1}{E - H_0 - \mathbf{V}_p - \mathbf{\Sigma}^r} \quad (12)$$

where $\mathbf{\Sigma}^r \equiv \sum_\alpha \mathbf{\Sigma}_\alpha^r$ is the self energy, and $\mathbf{\Gamma}_\alpha = -2Im[\mathbf{\Sigma}_\alpha^r]$ is the linewidth function. In above equations, $\mathbf{G}^{r,a,<}$ denotes a 2×2 matrix with matrix elements $G_{\sigma,\sigma'}^{r,a,<}$ and $\sigma = \uparrow, \downarrow$. $\mathbf{V}_p = V_p \mathbf{I}$ where \mathbf{I} is a 2×2 unit matrix in the spin space. In real space representation, V_p is a diagonal matrix describing the variation of the potential landscape due to the external pumping parameter V . The self-energies are given³⁴

$$\mathbf{\Sigma}_\alpha^r(E) = \hat{R}_\alpha \begin{pmatrix} \Sigma_{\alpha\uparrow}^r & 0 \\ 0 & \Sigma_{\alpha\downarrow}^r \end{pmatrix} \hat{R}_\alpha^\dagger \quad (13)$$

and

$$\mathbf{\Sigma}_\alpha^<(E) = i f_\alpha \hat{R}_\alpha \begin{pmatrix} \Gamma_{\alpha\uparrow}^0 & 0 \\ 0 & \Gamma_{\alpha\downarrow}^0 \end{pmatrix} \hat{R}_\alpha^\dagger \quad (14)$$

with the rotational matrix \hat{R}_α for electrode α defined as

$$\hat{R} = \begin{pmatrix} \cos \theta_\alpha/2 & \sin \theta_\alpha/2 \\ -\sin \theta_\alpha/2 & \cos \theta_\alpha/2 \end{pmatrix} \quad . \quad (15)$$

Here angle θ_α is defined as $\theta_L = 0$ and $\theta_R = \theta$ and $\Sigma_{\alpha\sigma}^r$ is given by

$$\Sigma_{\alpha\sigma mn}^r = \sum_k \frac{T_{k\alpha m}^* T_{k\alpha n}}{E - \epsilon_{k\alpha\sigma}^0 + i\delta} \quad (16)$$

and $\Gamma_{\alpha\sigma}^0 = -2Im(\Sigma_{\alpha\sigma}^r)$ is the linewidth function when $\theta = 0$.

In order for a parametric electron pump to function at low frequency, we need simultaneous variation of two or more system parameters controlled by gate voltages: $V_i(t) = V_{i0} + V_{ip} \cos(\omega t + \phi_i)$. Hence, in our case, the potential due to the gates can be written as $V_p = \sum_i V_i \Delta_i$, where Δ_i is potential profile due to each pumping potential. For simplicity we assume a constant gate potential such as that $(\Delta_1)_{xx}$ is one for x in the first gate region and zero otherwise. If the time variation of these parameters are slow, i.e. for $V(t) = V_0 + \delta V \cos(\omega t)$, then the charge of the system coming from all contacts due to the infinitesimal change of the system parameter ($\delta V \rightarrow 0$) is

$$dQ_p(t) = \sum_i \partial_{V_i} \text{Tr}[Q(x, t)] \delta V_i(t) \quad (17)$$

it is easily seen that the total charge in the system in a period is zero which is required for the charge conservation. To calculate the pumped current, we have to find the charge $dQ_{p\alpha}$ passing through contact α due to the change of the system parameters. Using the Dyson equation $\partial_{V_i} \mathbf{G}^r = \mathbf{G}^r \Delta_i \mathbf{G}^r$, the above equation becomes,

$$\begin{aligned} dQ_p(t) &= q \sum_j \int \frac{dE}{2\pi} \sum_\beta \text{Tr}[\mathbf{G}^r \Delta_j \mathbf{G}^r \mathbf{T}_\beta \mathbf{G}^a \\ &\quad + \mathbf{G}^r \mathbf{T}_\beta \mathbf{G}^a \Delta_j \mathbf{G}^a] f_\beta(E) \delta V_j(t) \\ &= -q \int \frac{dE}{2\pi} \sum_j \sum_\beta f_\beta \text{Tr}[\partial_E [\mathbf{G}^r \mathbf{T}_\beta \mathbf{G}^a \Delta_j]] \delta V_j(t) \end{aligned}$$

where the wideband limit has been taken. Integrating by part, we obtain

$$dQ_p(t) = q \int dE \sum_\beta (\partial_E f_\beta) \sum_j \frac{dN_\beta}{dV_j} \delta V_j(t) \quad (18)$$

where we have used the injectivity³⁹

$$\frac{dN_\beta}{dV_j} = \frac{1}{2\pi} \text{Tr}[\mathbf{G}^r \mathbf{T}_\beta \mathbf{G}^a \Delta_j] \quad (19)$$

Using the partial density of states $dN_{\alpha\beta}/dV_j$ defined as⁴⁰

$$\begin{aligned} \frac{dN_{\alpha\beta}}{dV_j} &= \frac{1}{4\pi} \text{Tr}[\mathbf{G}^r \mathbf{T}_\alpha \mathbf{G}^r \Delta_j + c.c.] \delta_{\alpha\beta} \\ &\quad + \frac{1}{4\pi} \text{Tr}[i \mathbf{G}^r \mathbf{T}_\beta \mathbf{G}^a \mathbf{T}_\alpha \mathbf{G}^r \Delta_j + c.c.] \end{aligned} \quad (20)$$

with $\sum_\alpha dN_{\alpha\beta}/dV_j = dN_\beta/dV_j$, we obtain

$$dQ_{p\alpha}(t) = -q \int dE \sum_\beta (-\partial_E f_\beta) \sum_j \frac{dN_{\alpha\beta}}{dV_j} \delta V_j(t) \quad (21)$$

If we include the charge passing through contact α due to the external bias, then

$$\begin{aligned} dQ_\alpha(t) &= -q \int dE \sum_\beta (-\partial_E f_\beta) \sum_j \frac{dN_{\alpha\beta}}{dV_j} \frac{dV_j(t)}{dt} dt \\ &\quad - q \int dE \sum_\beta \text{Tr}[\mathbf{T}_\alpha \mathbf{G}^r \mathbf{T}_\beta \mathbf{G}^a] (f_\alpha - f_\beta) dt \end{aligned} \quad (22)$$

Furthermore, the total current flowing through contact α due to both the variation of parameters V_j and external bias, in one period, is given by

$$J_\alpha = \frac{1}{\tau} \int_0^\tau dt dQ_\alpha/dt \quad (23)$$

where $\tau = 2\pi/\omega$ is the period of cyclic variation. If there are two pumping parameters, Eq.(23) can be written as when $\alpha = 1$,

$$\begin{aligned} J_1^{(1)} &= \frac{q}{2\tau} \int dt \int dE \partial_E (f_1 - f_2) \sum_j \\ &\quad \left[\frac{dN_{11}}{dV_j} \frac{dV_j(t)}{dt} - \frac{dN_{12}}{dV_j} \frac{dV_j(t)}{dt} \right] dt \\ &\quad - \frac{q}{\tau} \int dt \int dE \text{Tr}[\mathbf{T}_1 \mathbf{G}^r \mathbf{T}_2 \mathbf{G}^a] (f_1 - f_2) \end{aligned} \quad (24)$$

and

$$\begin{aligned} J_1^{(2)} &= \frac{q}{2\tau} \int dt \int dE \partial_E (f_1 + f_2) \sum_j \\ &\quad \left[\frac{dN_{11}}{dV_j} \frac{dV_j(t)}{dt} + \frac{dN_{12}}{dV_j} \frac{dV_j(t)}{dt} \right] dt \end{aligned} \quad (25)$$

where $J_1 = J_1^{(1)} + J_1^{(2)}$. In Ref. 22, $J_1^{(1)}$ has been identified as the current due to the external bias and $J^{(2)}$ as pumping current. For $\theta = 0, \pi$, all the 2×2 matrix are diagonal. In this case, it is easy to show that Eq.(23) agrees with the result of Ref. 22. If the external bias is zero, Eq.(23) reduces to the familiar formula¹ when there are two pumping potentials,

$$J_\alpha = \frac{q\omega}{2\pi} \int_0^\tau dt \left[\frac{dN_\alpha}{dX_1} \frac{dX_1}{dt} + \frac{dN_\alpha}{dX_2} \frac{dX_2}{dt} \right] \quad (26)$$

B. Finite frequency pumping in the weak pumping limit

In this subsection, we will calculate the pumping current at finite frequency. The Keldysh nonequilibrium Green's function approach used here is in the standard tight-binding representation³⁵. We could not use the momentum space version because the time dependent perturbation (pumping potential) inside the scattering region is position dependent. Hence it is most suitable to use a tight-binding real space technique. In contrast, in previous investigations³⁸ on photon-assisted processes the time-dependent potential is uniform throughout the dot and therefore a momentum space method is easier to apply.

Assuming the time-dependent perturbations located at the different sites, $j = i_0, j_0$, and k_0 etc, with

$$V_j(t) = V_j \cos(\omega t + \phi_j) \quad (27)$$

When there is no interaction between electrons in the ideal leads L and R , the standard nonequilibrium Green's function theory gives the following expression for the time dependent current³⁶,

$$J_\alpha(t) = -q \int_{-\infty}^t dt_1 \text{Tr}[\mathbf{G}^r(t, t_1) \Sigma_\alpha^<(t_1, t) + \mathbf{G}^<(t, t_1) \Sigma_\alpha^a(t_1, t) + c.c.] \quad (28)$$

and transmission coefficient

$$T(E) = \text{Tr}[\mathbf{\Gamma}_L^r(E) \mathbf{G}^r(E) \mathbf{\Gamma}_R^r(E) \mathbf{G}^a(E)] \quad (29)$$

where the scattering Green's functions and self-energy are defined in the usual manner:

$$\mathbf{G}_{ij\sigma\sigma'}^{r,a}(t_1, t_2) = \mp i\theta(\pm t_1 \mp t_2) \langle \{d_{i,\sigma}(t_1), d_{j,\sigma'}^\pm(t_2)\} \rangle \quad (30)$$

$$\mathbf{G}_{ij,\sigma,\sigma'}^<(t_1, t_2) = i \langle d_{j,\sigma'}^+(t_2) d_{i,\sigma}(t_1) \rangle \quad (31)$$

$$\Sigma_{\alpha ij}^{r,a,<}(t_1, t_2) = \sum_k T_{\alpha ki}^* T_{\alpha kj} \mathbf{g}_\alpha^{r,a,<}(t_1, t_2) \quad (32)$$

The average current $J_L(t)$ from the left lead can be written as

$$\begin{aligned} \langle J_L(t) \rangle &= -\frac{q}{\tau} \int_0^\tau dt \int_{-\infty}^t dt_1 \text{Tr}[\mathbf{G}_{11}^r(t, t_1) \Sigma_L^<(t_1, t) \\ &+ \mathbf{G}_{11}^<(t, t_1) \Sigma_L^a(t_1, t) + c.c.] \end{aligned} \quad (33)$$

In the absence of pumping, the retarded Green's function is defined in terms of the Hamiltonian H_0 ,

$$\mathbf{G}^{0r}(E) = \frac{1}{E - H_0 - \Sigma^r} \quad (34)$$

and $\mathbf{G}^{0<}$ is related to the retarded and advanced Green's functions \mathbf{G}^{0r} and \mathbf{G}^{0a} by,

$$\mathbf{G}^{0<}(E) = \mathbf{G}^{0r}(E) \Sigma^<(E) \mathbf{G}^{0a}(E) \quad (35)$$

Now we make use of the time-dependent pumping potentials $V_j(t)$ as the perturbations to calculate all kinds of Green's functions up to the second order, and corresponding average current.

First, we calculate the current corresponding to the term $\mathbf{G}_{11}^r(t, t_1) \Sigma_L^<(t_1, t)$ in Eq.(33). Dyson equation for $\mathbf{G}_{11}^r(t, t_1)$ gives the second order contribution:

$$\begin{aligned} \mathbf{G}_{11}^{(2)r}(t, t_1) &= \sum_{jk} \int \int dx dy \mathbf{G}_{1j}^{0r}(t - x) \\ &\mathbf{V}_j(x) \mathbf{G}_{jk}^{0r}(x - y) \mathbf{V}_k(y) \mathbf{G}_{k1}^{0r}(y - t_1) \\ &\equiv \sum_{jk} \mathbf{G}_{1j}^{0r} \mathbf{V}_j \mathbf{G}_{jk}^{0r} \mathbf{V}_k \mathbf{G}_{k1}^{0r} \end{aligned} \quad (36)$$

Substituting Eq.(36) into Eq.(33) and completing the integration over time x, y, t_1, t , it is not difficult to calculate the average current $\langle J_{L1} \rangle$ due to the first term in Eq.(33) (see appendix for details),

$$\begin{aligned} \langle J_{L1}(t) \rangle &= - \sum_{jk} \frac{qV_j V_k}{4} \int \frac{dE}{2\pi} \text{Tr} [\Sigma_L^< \mathbf{G}_{1j}^{0r} \\ &[\mathbf{G}_{jk}^{0r}(E_-) e^{i\Delta_{kj}} + \mathbf{G}_{jk}^{0r}(E_+) e^{-i\Delta_{kj}}] \mathbf{G}_{k1}^{0r}] \end{aligned} \quad (37)$$

where $\Delta_{kj} = \phi_k - \phi_j$ is the phase difference, $E_\pm = E \pm \omega$, and $G^{r,a,<} \equiv G^{r,a,<}(E)$.

Now we calculate the second term $\mathbf{G}_{11}^<(t, t_1) \Sigma_L^a(t_1, t)$ in Eq.(33). Using Keldysh equation, $\mathbf{G}^< = \mathbf{G}^r \Sigma^< \mathbf{G}^a$, we have

$$\mathbf{G}_{jk}^< = \mathbf{G}_{j1}^r \Sigma_L^< \mathbf{G}_{1k}^a + \mathbf{G}_{jN}^r \Sigma_R^< \mathbf{G}_{Nk}^a \quad (38)$$

where $\Sigma_\alpha^< = i\mathbf{\Gamma}_\alpha f_\alpha$. Expanding $G^{r,a}$ up to the second order in pumping parameters, we obtain the second order contribution from $\mathbf{G}_{11}^<$,

$$\begin{aligned} \mathbf{G}_{11}^{(2)<} &= \mathbf{G}_{11}^r \Sigma_L^< \mathbf{G}_{11}^a + \mathbf{G}_{1N}^r \Sigma_R^< \mathbf{G}_{N1}^a \\ &= \mathbf{G}_{11}^{(2)r} \Sigma_L^< \mathbf{G}_{11}^{0a} + \mathbf{G}_{11}^{(1)r} \Sigma_L^< \mathbf{G}_{11}^{(1)a} + \mathbf{G}_{11}^{0r} \Sigma_L^< \mathbf{G}_{11}^{(2)a} \\ &+ \mathbf{G}_{1N}^{(2)r} \Sigma_R^< \mathbf{G}_{N1}^{0a} + \mathbf{G}_{1N}^{(1)r} \Sigma_R^< \mathbf{G}_{N1}^{(1)a} + \mathbf{G}_{1N}^{0r} \Sigma_R^< \mathbf{G}_{N1}^{(2)a} \\ &= \sum_{jk} [\mathbf{G}_{1j}^{0r} \mathbf{V}_j \mathbf{G}_{jk}^{0r} \mathbf{V}_k \mathbf{G}_{k1}^{0<} + \mathbf{G}_{1j}^{0r} \mathbf{V}_j \mathbf{G}_{jk}^{0<} \mathbf{V}_k \mathbf{G}_{k1}^{0a} \\ &+ \mathbf{G}_{1j}^{0<} \mathbf{V}_j \mathbf{G}_{jk}^{0a} \mathbf{V}_k \mathbf{G}_{k1}^{0a}] \end{aligned} \quad (39)$$

where we have used Eq.(38) to simplify the expression. After some algebra, we have the following three expressions corresponding to each term in Eq.(39),

$$\begin{aligned} &- \sum_{jk} \frac{qV_j V_k}{4} \int \frac{dE}{2\pi} \text{Tr} [\Sigma_L^a \mathbf{G}_{1j}^{0r} \\ &[\mathbf{G}_{jk}^{0r}(E_-) e^{i\Delta_{kj}} + e^{-i\Delta_{kj}} \mathbf{G}_{jk}^{0r}(E_+)] \mathbf{G}_{k1}^{0<}] \end{aligned} \quad (40)$$

$$\begin{aligned} &- \sum_{jk} \frac{qV_j V_k}{4} \int \frac{dE}{2\pi} \text{Tr} [\Sigma_L^a \mathbf{G}_{1j}^{0r} \\ &[\mathbf{G}_{jk}^{0<}(E_-) e^{i\Delta_{kj}} + e^{-i\Delta_{kj}} \mathbf{G}_{jk}^{0<}(E_+)] \mathbf{G}_{k1}^{0a}] \end{aligned} \quad (41)$$

$$\begin{aligned} &- \sum_{jk} \frac{qV_j V_k}{4} \int \frac{dE}{2\pi} \text{Tr} [\Sigma_L^a \mathbf{G}_{1j}^{0<} \\ &[\mathbf{G}_{jk}^{0a}(E_-) e^{i\Delta_{kj}} + e^{-i\Delta_{kj}} \mathbf{G}_{jk}^{0a}(E_+)] \mathbf{G}_{k1}^{0a}] \end{aligned} \quad (42)$$

The final pumped current is the sum of Eq.(37), (40), (41), (42) and their complex conjugates, in addition to the current directly due to the external bias (see second term of Eq.(24)). If the external bias is zero, the expression of the pumped current can be simplified significantly. Note that in the equilibrium, the lesser Green's function satisfies the fluctuation-dissipation theorem,

$$\mathbf{G}^{0<}(E) = -f(E) [\mathbf{G}^{0r}(E) - \mathbf{G}^{0a}(E)] \quad (43)$$

and

$$\mathbf{G}^{0<}(E_\pm) = -f(E_\pm) [\mathbf{G}^{0r}(E_\pm) - \mathbf{G}^{0a}(E_\pm)] \quad (44)$$

(37)+(40)+(42)* leads to

$$-i \sum_{jk} \frac{qV_j V_k}{4} \int \frac{dE}{2\pi} \text{Tr} [\mathbf{\Gamma}_L \mathbf{G}_{1j}^{0r} f(E) [\mathbf{G}_{jk}^{0r}(E_-) e^{i\Delta_{kj}} + e^{-i\Delta_{kj}} \mathbf{G}_{kj}^{0r}(E_+)] \mathbf{G}_{k1}^{0a}] \quad (45)$$

while (37)*+(40)*+(42) gives to

$$i \sum_{jk} \frac{qV_j V_k}{4} \int \frac{dE}{2\pi} \text{Tr} [\mathbf{\Gamma}_L \mathbf{G}_{1j}^{0r} f(E) [\mathbf{G}_{jk}^{0a}(E_-) e^{i\Delta_{kj}} + e^{-i\Delta_{kj}} \mathbf{G}_{kj}^{0a}(E_+)] \mathbf{G}_{k1}^{0a}] \quad (46)$$

furthermore, (41)+c.c. becomes

$$i \sum_{jk} \frac{qV_j V_k}{4} \int \frac{dE}{2\pi} \text{Tr} [\mathbf{\Gamma}_L \mathbf{G}_{1j}^{0r} [f_-(\mathbf{G}_{jk}^{0r}(E_-) - \mathbf{G}_{jk}^{0a}(E_-)) e^{i\Delta_{kj}} + e^{-i\Delta_{kj}} f_+(\mathbf{G}_{jk}^{0r}(E_+) - \mathbf{G}_{jk}^{0a}(E_+))] \mathbf{G}_{k1}^{0a}] \quad (47)$$

where $f_{\pm} = f(E_{\pm})$.

Combining Eqs.(45), (46) and (47), we finally obtain

$$J_L = i \sum_{jk} \frac{qV_j V_k}{4} \int \frac{dE}{2\pi} \text{Tr} [\mathbf{\Gamma}_L \mathbf{G}_{1j}^{0r} [(f_- - f)(\mathbf{G}_{jk}^{0r}(E_-) - \mathbf{G}_{jk}^{0a}(E_-)) e^{i\Delta_{kj}} + e^{-i\Delta_{kj}} (f_+ - f)(\mathbf{G}_{jk}^{0r}(E_+) - \mathbf{G}_{jk}^{0a}(E_+))] \mathbf{G}_{k1}^{0a}] \quad (48)$$

In the limit of small frequency, we expand Eq.(48) up to the first order in frequency and use the fact that

$$\mathbf{G}^{0r} - \mathbf{G}^{0a} = -i\mathbf{G}^{0r}\mathbf{\Gamma}\mathbf{G}^{0a} \quad (49)$$

and Dyson equation,

$$\mathbf{G}_{ji}^{0r} \mathbf{G}_{ik}^{0r} = \frac{\partial \mathbf{G}_{jk}^{0r}}{\partial \mathbf{V}_i} \quad (50)$$

we obtain,

$$J_L = \sum_{jk} \frac{q\omega V_j V_k \sin(\Delta_{kj})}{2} \int \frac{dE}{2\pi} \partial_E f(E) \text{Tr} \{ \mathbf{\Gamma}_L \mathbf{G}_{1j}^{0r}(E) [\mathbf{G}_{jk}^{0r}(E) - \mathbf{G}_{jk}^{0a}(E)] \mathbf{G}_{k1}^{0a}(E) \} \\ = - \sum_{jk} \frac{i q \omega V_j V_k \sin(\Delta_{jk})}{2} \int \frac{dE}{2\pi} \partial_E f(E) \text{Tr} \left[\mathbf{\Gamma}_L \frac{\partial \mathbf{G}_{11}^{0r}}{\partial \mathbf{V}_j} \mathbf{\Gamma}_L \frac{\partial \mathbf{G}_{11}^{0a}}{\partial \mathbf{V}_k} + \mathbf{\Gamma}_L \frac{\partial \mathbf{G}_{12}^{0r}}{\partial \mathbf{V}_j} \mathbf{\Gamma}_R \frac{\partial \mathbf{G}_{21}^{0a}}{\partial \mathbf{V}_k} \right] \quad (51)$$

which is the same as Ref. 1 when $\theta = 0$.

III. RESULTS

We now apply our formula Eqs.(24), (25) and (48) to a TMR junction. For current perpendicular to the plane

geometry, the TMR junction can be modeled by an one-dimensional quantum structure with a double barrier potential $U(x) = X_1 \delta(x+a) + X_2 \delta(x-a)$ where $2a$ is the well width. For this system the Green's function $G(x, x')$ can be calculated exactly⁴². The adiabatic pump that we consider is operated by changing barrier heights adiabatically and periodically: $X_1 = V_0 + V_p \sin(\omega t)$ and $X_2 = V_0 + V_p \sin(\omega t + \phi)$. In the following, we will study zero temperature behavior of the pumped current. In the calculation, we have chosen $M = 37.0$ and $V_0 = 79.2$. Finally the unit is set by $\hbar = 2m = 1$ ⁴¹.

We first study the pumped current with two pumping potentials in the adiabatic regime. Fig.1 depicts the transmission coefficient T versus Fermi energy at several angles θ . As expected, among different angles, T is the largest at $\theta = 0$ and smallest at $\theta = \pi$ with the ratio $T_{max}(0)/T_{max}(\pi) \sim 4$. This gives the usual spin valve effect³¹. Fig.2 plots the pumped current versus Fermi energy at different θ . Here we have set the phase difference of two pumping potentials to be $\pi/2$. Similar to the transmission coefficient, we obtain largest pumped current at $\theta = 0$ and smallest current at $\theta = \pi$. We found that the ratio $I_{max}(0)/I_{max}(\pi)$ is about the same as that of transmission coefficient. As the pumping amplitude doubles, the peak of pumped current is broadened and the maximum pumped current is doubled (see inset of Fig.2). This is understandable since at large pumping amplitude the instantaneous resonant level oscillates with a large amplitude and hence can generate heat current in a broad range of energy. The spin valve effect of pumped current is illustrated in Fig.3 where the pumped current versus θ is shown when the system is at resonance. We see that the pumped current is maximum at $\theta = 0$ and decreases quickly as one increases θ from 0 to π . For larger pumping amplitude, we have similar behavior (inset of Fig.3). In Fig.4, we plot the pumped current as a function of phase difference ϕ between two pumping potentials. We see that the pumped current is antisymmetric about the $\phi = \pi$. The nonlinear behavior is clearly seen which deviates from the sinusoidal behavior at small pumping amplitude. In Fig.5, we show the pumped current in the presence of external bias. In the calculation we assume that $V_L = -\omega V/2$ and $V_R = \omega V/2$ so that the external bias is against the pumped current when V is positive. Due to the external bias, the total pumped current (dashed line) decreases near resonant energy and reverses the direction at other energies. Now we turn to the case of finite frequency pumping. We first present our results (Fig.6 to Fig.8) at small pumping frequency $\omega = 0.002$. In Fig.6 we plot the pumped current as a function of phase difference ϕ near the resonant energy. At $\theta = 0$, the magnitude of pumped current is much larger than that at $\theta = \pi/2$ or π . We notice that at $\phi = 0$ and $\phi = \pi$, the pumped current is nonzero similar to the experimental anomaly observed experimentally for nonmagnetic system³. The pumped current away from resonant energy is shown in Fig.7. At $\theta = 0$, we see that the pumped current is sharply peaked at resonant

energy. The pumped current is positive for $\phi = \pi/2$ and negative for $\phi = 0$ and π . At $\theta = \pi/2$ or π , the pumped current at $\phi = \pi/2$ (dashed line) is much larger than that at other angles. Fig.8 displays the pumped current as a function of θ near resonant energy. For $\phi = \pi/2$ (dotted line), we see the usual behavior that large pumped current occurs at $\theta = 0$ and it decreases to the minimum at $\theta = \pi$. For $\phi = 0$ or π , however, we see completely different behavior. The pumped current is still the largest at $\theta = 0$ but the direction of the pumped current is reversed. As one increases θ , the pumped current decreases and reaches a flat region with almost zero pumped current. Now we study the effect of frequency to the pumped current versus θ (see Fig.9). We will fix the phase difference to be $\phi = \pi/2$ and energy near resonance. At small frequency $\omega = 0.002$ (dashed line), the pumped current versus θ show usual behavior. When the frequency is increased to $\omega = 0.004$ (dot-dashed line), two peaks show up symmetrically near $\theta = \pm\pi/4$ while the minimum is still at $\theta = \pi$. As frequency is increased further to $\omega = 0.006$ (dotted line), the pumped current near $\theta = 0$ reverses the direction and the new peak position shifts to $\theta \sim 0.35\pi$. Upon further increasing ω , the curve of pumped current versus θ develops a flat region between $\theta = \pm 0.35\pi$ with positive current while the magnitude of the negative pumped current at $\theta = 0$ becomes larger (see Fig.9b). Finally, at even larger frequency $\omega = 0.1$, all the pumped currents are negative. This behavior can be understood from the photon assisted process¹⁹. The quantum interference between contributions due to photon emission (or absorption) near two pumping potentials is essential to understand the nature of pumped current. In addition to the interference effect, the pumped current is also affected by a competition of between the photon emission and absorption processes which tend to cancel to each other. It is the interplay between this competition and interference that gives rise to the interesting spin valve effect for the pumped current. Finally, we show in Fig.10 the pumped current versus pumping frequency. We see that at small frequency the current is positive and small, at large frequency the current is much large and is negative.

In summary, we have developed a general theory for parametric pumping in the presence of ferromagnetic leads. Our theory is based on the nonequilibrium Green's function method and is valid for multi-modes (in two or three dimensions) and can be easily extended to the case of multi-probes (although most of calculations are for two probes). In the parametric pumping, two kinds of driving forces are present: multiple pumping potentials inside the scattering system as well as the external bias in the multi-probes. Two cases are considered. In the adiabatic regime, the system is in near equilibrium. In this case our theory is for general pumping amplitude. At finite frequency, the system is away from equilibrium. Our theory is up the quadratic order in pumping amplitude. This theory allows us to examine the pumped current in broader parameter space including pumping amplitude,

pumping frequency, phase difference between two pumping potentials, the angle between magnetization of two leads.

ACKNOWLEDGMENTS

We gratefully acknowledge support by a RGC grant from the SAR Government of Hong Kong under grant number HKU 7091/01P.

IV. APPENDIX

Now we show that

$$\begin{aligned} B &\equiv \frac{1}{\tau} \int_0^\tau dt \int_{-\infty}^t dt_1 \text{Tr}[\mathbf{F}_0(t_1, t) \mathbf{G}(t, t_1)] \\ &= \frac{V_\alpha V_\beta}{4} \int \frac{dE}{2\pi} \text{Tr} [\mathbf{F}_0(E) \mathbf{F}_1(E) [\mathbf{F}_2(E_+) e^{i\Delta_{\beta\alpha}} \\ &\quad + e^{-i\Delta_{\beta\alpha}} \mathbf{F}_2(E_-)] \mathbf{F}_3(E)] \end{aligned} \quad (52)$$

where

$$\mathbf{G} \equiv \mathbf{F}_1 \mathbf{V}_\alpha \mathbf{F}_2 \mathbf{V}_\beta \mathbf{F}_3 \quad (53)$$

and F_i 's ($i = 0, 1, 2, 3$) satisfy $F_i(t_1, t_2) = F_i(t_1 - t_2)$.

Taking the Fourier transform,

$$\mathbf{F}(t) = \frac{1}{2\pi} \int dE e^{-iEt} \mathbf{F}(E) \quad (54)$$

we obtain

$$\begin{aligned} B &= \frac{1}{\tau} \int_0^\tau dt \int_{-\infty}^t dt_1 \int \frac{dE}{2\pi} \mathbf{F}_0(E) e^{-iE(t_1-t)} \int dx dy \\ &\quad [\mathbf{F}_1(t-x) V_\alpha(x) \mathbf{F}_2(x-y) V_\beta(y) \mathbf{F}_3(y-t_1)] \\ &= \frac{1}{\tau} \int_0^\tau dt \int \prod_{i=1,5} \frac{dE_i}{2\pi} \int \frac{dE}{2\pi} \int_{-\infty}^t dt_1 \int dx dy \\ &\quad \mathbf{F}_0(E) \mathbf{F}_1(E_1) \mathbf{V}_\alpha(E_2) \mathbf{F}_2(E_3) \mathbf{V}_\beta(E_4) \mathbf{F}_3(E_5) \\ &\quad e^{i(E-E_1)t} e^{i(E_5-E)t_1} e^{i(E_1-E_2-E_3)x} e^{i(E_3-E_4-E_5)y} \end{aligned}$$

where

$$\mathbf{V}_\alpha(E) = \pi V_\alpha [e^{i\phi_\alpha} \delta(E_+) + e^{-i\phi_\alpha} \delta(E_-)] \quad (55)$$

Integrating over x and y yields,

$$\begin{aligned} B &= \frac{1}{\tau} \int_0^\tau dt \int \prod_{i=1,5} \frac{dE_i}{2\pi} \int \frac{dE}{2\pi} \int_{-\infty}^t dt_1 \mathbf{F}_0(E) \\ &\quad \mathbf{F}_1(E_1) \mathbf{V}_\alpha(E_2) \mathbf{F}_2(E_3) \mathbf{V}_\beta(E_4) \mathbf{F}_3(E_5) e^{i(E-E_1)t} \\ &\quad e^{i(E_5-E)t_1} (2\pi)^2 \delta(E_1-E_2-E_3) \delta(E_5-E_4-E_5) \end{aligned}$$

Integrating over t_1, t and using Eq.(55), we have

$$\begin{aligned}
B &= \int \frac{dE_2}{2\pi} \frac{dE_4}{2\pi} \frac{dE_5}{2\pi} \int \frac{dE}{2\pi} \frac{\mathbf{F}_0(E)}{i[E_5 - E - i\delta]} \\
&\mathbf{F}_1(E_2 + E_4 + E_5) \mathbf{V}_\alpha(E_2) \mathbf{F}_2(E_4 + E_5) \\
&\mathbf{V}_\beta(E_4) \mathbf{F}_3(E_5) \delta(E_2 + E_4) \\
&= \frac{V_\alpha V_\beta}{4} \int \frac{dE_5}{2\pi} \frac{dE}{2\pi} \frac{\mathbf{F}_0(E)}{i[E_5 - E - i\delta]} \mathbf{F}_1(E_5) \\
&[\mathbf{F}_2(E_5 + \omega) e^{i\Delta_{\beta\alpha}} + e^{-i\Delta_{\beta\alpha}} \mathbf{F}_2(E_5 - \omega)] \mathbf{F}_3(E_5)
\end{aligned}$$

Using the theorem of residue, we have

$$\int dE \frac{F_0(E)}{i[E_5 - E - i\delta]} = 2\pi F_0(E_5) \quad (56)$$

we thus obtain Eq.(52).

^{a)} Electronic mail: jianwang@hkusub.hku.hk

¹ P.W. Brouwer, Phys. Rev. B **58**, R10135 (1998).

² I.L. Aleiner and A.V. Andreev, Phys. Rev. Lett. **81**, 1286 (1998).

³ M. Switkes, C. Marcus, K. Capman, and A.C. Gossard, Science **283**, 1905 (1999).

⁴ F. Zhou, B. Spivak, and B.L. Altshuler, Phys. Rev. Lett. **82**, 608 (1999).

⁵ T.A. Shutenko, I.L. Aleiner, and B.L. Altshuler, Phys. Rev. B **61**, 10366 (2000).

⁶ Y.D. Wei, J. Wang, and H. Guo, Phys. Rev. B **62**, 9947 (2000).

⁷ I.L. Aleiner, B.L. Altshuler, and A. Kamenev, Phys. Rev. B **62**, 10373 (2000).

⁸ J.E. Avron, A. Elgart, G.M. Graf, and L. Sadun, Phys. Rev. B **62**, R10618 (2000).

⁹ Y. Levinson, O. Entin-Wohlman, and P. Wolffe, Physica A **302**, 335 (2001).

¹⁰ P.W. Brouwer, Phys. Rev. B **63**, 121303 (2001); M.L. Polianski and P.W. Brouwer, Phys. Rev. B **64**, 075304 (2001).

¹¹ M. Moskalets and M. Buttiker, Phys. Rev. B **64**, 201305 (2001).

¹² J.E. Avron, A. Elgart, G.M. Graf, and L. Sadun, Phys. Rev. Lett. **87**, 236601 (2001).

¹³ J. Wang et al, Appl. Phys. Lett. **79**, 3977 (2001).

¹⁴ M.G. Vavilov, V. Ambegaokar, and I.L. Aleiner, Phys. Rev. B **63**, 195313 (2001).

¹⁵ Y.D. Wei, J. Wang, H. Guo, and C. Roland, Phys. Rev. B **64**, 115321 (2001).

¹⁶ F. Renzoni and T. Brandes, Phys. Rev. B **64**, 245301 (2001).

¹⁷ Y. Makhlin and A.D. Mirlin, Phys. Rev. Lett. **87**, 276803 (2001).

¹⁸ C.S. Tang and C.S. Chu, Solid State Comm. **120**, 353 (2001).

¹⁹ B.G. Wang, J. Wang, and H. Guo, Phys. Rev. B **65**, 073306 (2002).

²⁰ J. Wang and B.G. Wang, Phys. Rev. B **65**, 153311 (2002).

²¹ Y. Levinson, O. Entin-Wohlman, and P. Wolffe, cond-mat/0104408.

²² O. Entin-Wohlman, A. Aharony, and Y. Levinson, cond-mat/0201073.

²³ M. Moskalets and M. Buttiker, cond-mat/0201259.

²⁴ M.L. Polianski, M.G. Vavilov, and P.W. Brouwer, cond-mat/0202241.

²⁵ O. Entin-Wolman and A. Aharony, cond-mat/0202289.

²⁶ B.G. Wang and J. Wang, cond-mat/0203581.

²⁷ B.G. Wang and J. Wang, cond-mat/0204067.

²⁸ M. Blaauboer, cond-mat/0204340.

²⁹ J.L. Wu, B.G. Wang, and J. Wang, unpublished.

³⁰ R. Meservey and P.M. Tedrow, Phys. Rep. **238**, 173 (1994); M. Baibich *et al.*, Phys. Rev. Lett. **61**, 2472 (1988); G.A. Prinz, Science, **282**, 1660 (1998); D.J. Monsma, J.C. Lodder, Th.J.A. Popma, and B. Dieny, Phys. Rev. Lett. **74**, 5260 (1995); D.J. Monsma, R. Vlutters, J.C. Lodder, Science, **281**, 407 (1998); A. Wolf et al, Science **294**, 1488 (2001).

³¹ J.C. Slonczewski, Phys. Rev. B **39**, 6995 (1989).

³² J.S. Moodera, L.R. Kinder, T.M. Wong, and R. Meservey, Phys. Rev. Lett. **74**, 3273 (1995); S. Zhang, P.M. Levy, A.C. Marley and S.S.P. Parkin, Phys. Rev. Lett. **79**, 3744 (1997); X.D. Zhang, B.Z. Li, G. Sun, F.C. Pu, Phys. Rev. B **56**, 5484 (1997); J.S. Moodera, J. Nowak and R.J.M. van de Veerdonk, Phys. Rev. Lett. **80**, 2941 (1998); J. Barnaś and A. Fert, Phys. Rev. Lett. **80**, 1058 (1998); L. Sheng, Y. Chen, H.Y. Teng, and C.S. Ting, Phys. Rev. B **59**, 480 (1999); K. Tsukagoshi, B.W. Alphenaar, and H. Ago, Nature, **401**, 572 (1999); H. Mehrez et al, Phys. Rev. Lett. **84**, 2682 (2000).

³³ N.N. Bogoliubov, J. Phys. USSR, **11**, 23(1947).

³⁴ B.G. Wang, J. Wang, and H. Guo, J. Phys. Soc. Jpn. **70**, 2645 (2001).

³⁵ M. P. Anantram and S. Datta, Phys. Rev. B **51**, 7632 (1995).

³⁶ A.P. Jauho, N.S. Wingreen, and Y. Meir, Phys. Rev. B **50**, 5528 (1994).

³⁷ B.G. Wang, J. Wang, and H. Guo, Phys. Rev. Lett. **82**, 398 (1999); J. Appl. Phys. **86**, 5094 (1999).

³⁸ C.A. Stafford and N.S. Wingreen, Phys. Rev. Lett. **76**, 1916(1996). Q.F. Sun, J. Wang, T.H. Lin, Phys. Rev. B **58**, 13007 (1998); Phys. Rev. B **59**, 13126 (1999); Phys. Rev. B **61**, 12643, (2000). H.K. Zhao and J. Wang, Europhys. J. B **9**, 513 (1999).

³⁹ M. Büttiker, J. Phys. Condens. Matter **5**, 9361 (1993).

⁴⁰ T. Gramspacher and M. Büttiker, Phys. Rev. B **56**, 13026 (1997).

⁴¹ For the system of Fe/Ge/Fe with $a = 100\text{\AA}$, the energy unit is $E = 4.64\text{meV}$ which corresponds to frequency $\omega = 1.1 \times 10^{12}$ Hz. The unit of the pumped current in the adiabatic regime depends on the pumping frequency ω . If $\omega = 100\text{MHz}$, then the pumped current is $1.6 \times 10^{-11}\text{A}$. For pumped current at finite frequency, the unit of current is $2 \times 10^{-6}\text{A}$.

⁴² M.K. Yip, J. Wang, and H. Guo, Z. Phys. B: Condens. Matter **104**, 463 (1997).

FIG. 1. The transmission coefficient as a function of Fermi energy at different angle θ between the magnetizations of two leads: $\theta = 0$ (dashed line), $\theta = \pi/2$ (solid line), and $\theta = \pi$ (dotted line).

FIG. 2. The pumped current as a function of Fermi energy at different θ : $\theta = 0$ (solid line), $\theta = \pi/2$ (dot-dashed line), and $\theta = \pi$ (dotted line). Other parameters are $\phi = \pi/2$ and $V_p = 0.05V_0$. Inset: the same as the main figure except $V_p = 0.1V_0$.

FIG. 3. The pumped current as a function of θ . Here $\phi = \pi/2$, $E_F = 37.55$ and $V_p = 0.05V_0$. Inset: the same as main figure except $V_p = 0.1V_0$.

FIG. 4. The pumped current as a function of phase difference ϕ at different θ . $\theta = 0$ (dashed line), $\theta = \pi/2$ (dotted line), and $\theta = \pi$ (solid line). Other parameters are $E_F = 37.55$ and $V_p = 0.05V_0$.

FIG. 5. The pumped current as a function of Fermi energy with an external bias $V_L - V_R = -0.02\omega$ at different θ : (a). $\theta = \pi$. (b). $\theta = \pi/2$. (c). $\theta = 0$. In (a), (b) and (c), solid line: pumped current, dotted line: current due to external bias, dashed line: total current. Here $\phi = \pi/2$ and $V_p = 0.05V_0$.

FIG. 6. The pumped current as a function of ϕ at finite frequency. Dashed line: $\theta = 0$, dotted line: $\theta = \pi/2$, solid line: $\theta = \pi$. Here $E_F = 37.55$ and $\omega = 0.002$.

FIG. 7. The pumped current as a function of Fermi energy at finite frequency at different θ : (a). $\theta = 0$. (b). $\theta = \pi/2$. (c). $\theta = \pi$. In (a), (b) and (c), dotted line: $\phi = 0$, dashed line: $\phi = \pi/2$, solid line: $\phi = \pi$. Here $\omega = 0.002$.

FIG. 8. The pumped current as a function of θ at finite frequency. Here dashed line: $\phi = 0$, dotted line: $\phi = \pi/2$, solid line: $\phi = \pi$. Other parameters are $E_F = 37.55$ and $\omega = 0.002$.

FIG. 9. The pumped current as a function of θ at different frequencies. (a). $\omega = 0.002$ (short dashed line), 0.004 (dot-dashed line), 0.006 (dotted line), 0.008 (solid line). (b). $\omega = 0.01$ (solid line), 0.02 (dot-dashed line), 0.05 (short dashed line), 0.1 (dotted line). Other parameters are $E_F = 37.55$ and $\phi = \pi/2$.

FIG. 10. The pumped current as a function of frequency. Here $\theta = 0$, $\phi = \pi/2$ and $E_F = 37.55$.

Fig1

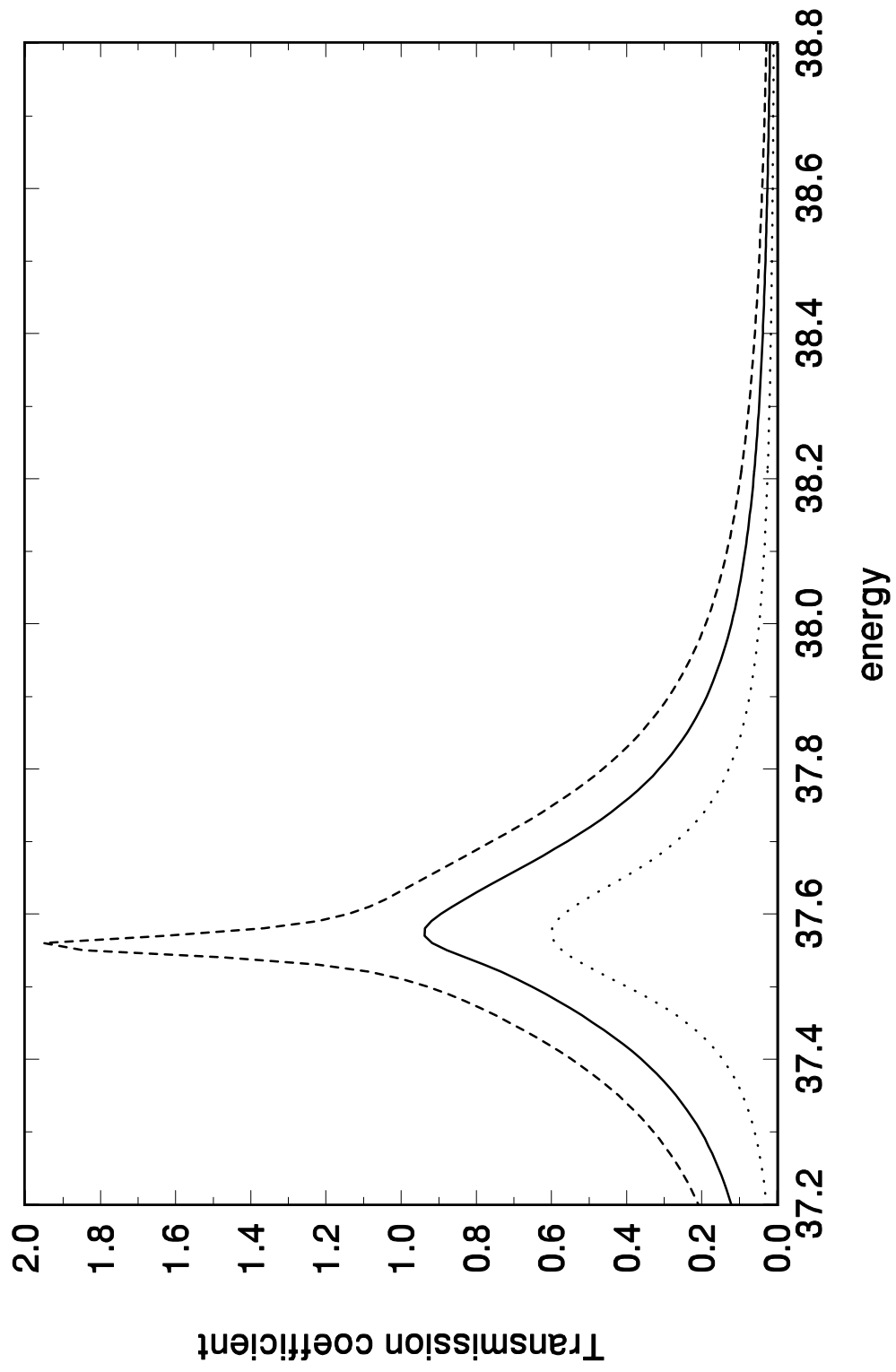


Fig2

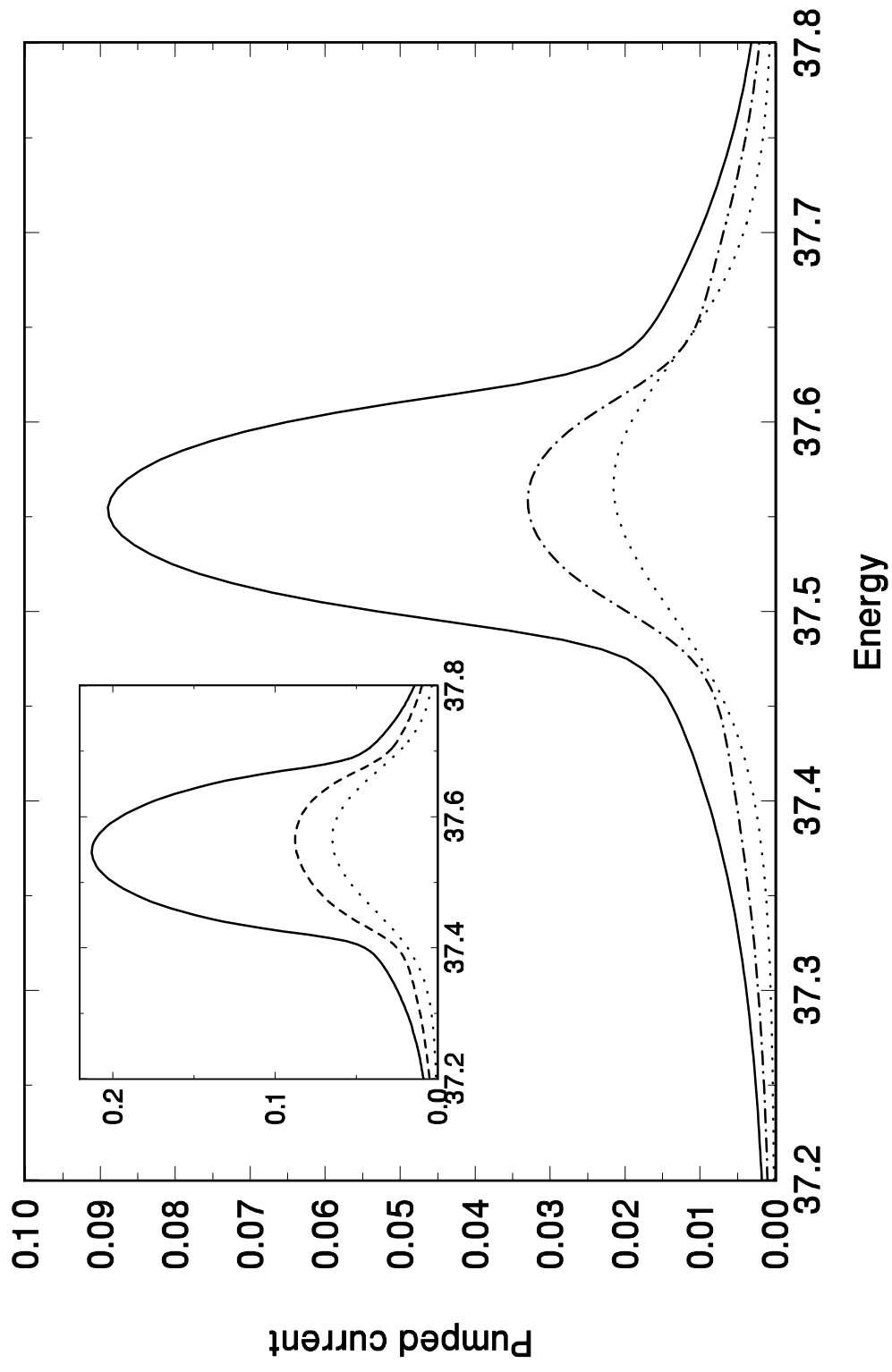


Fig3

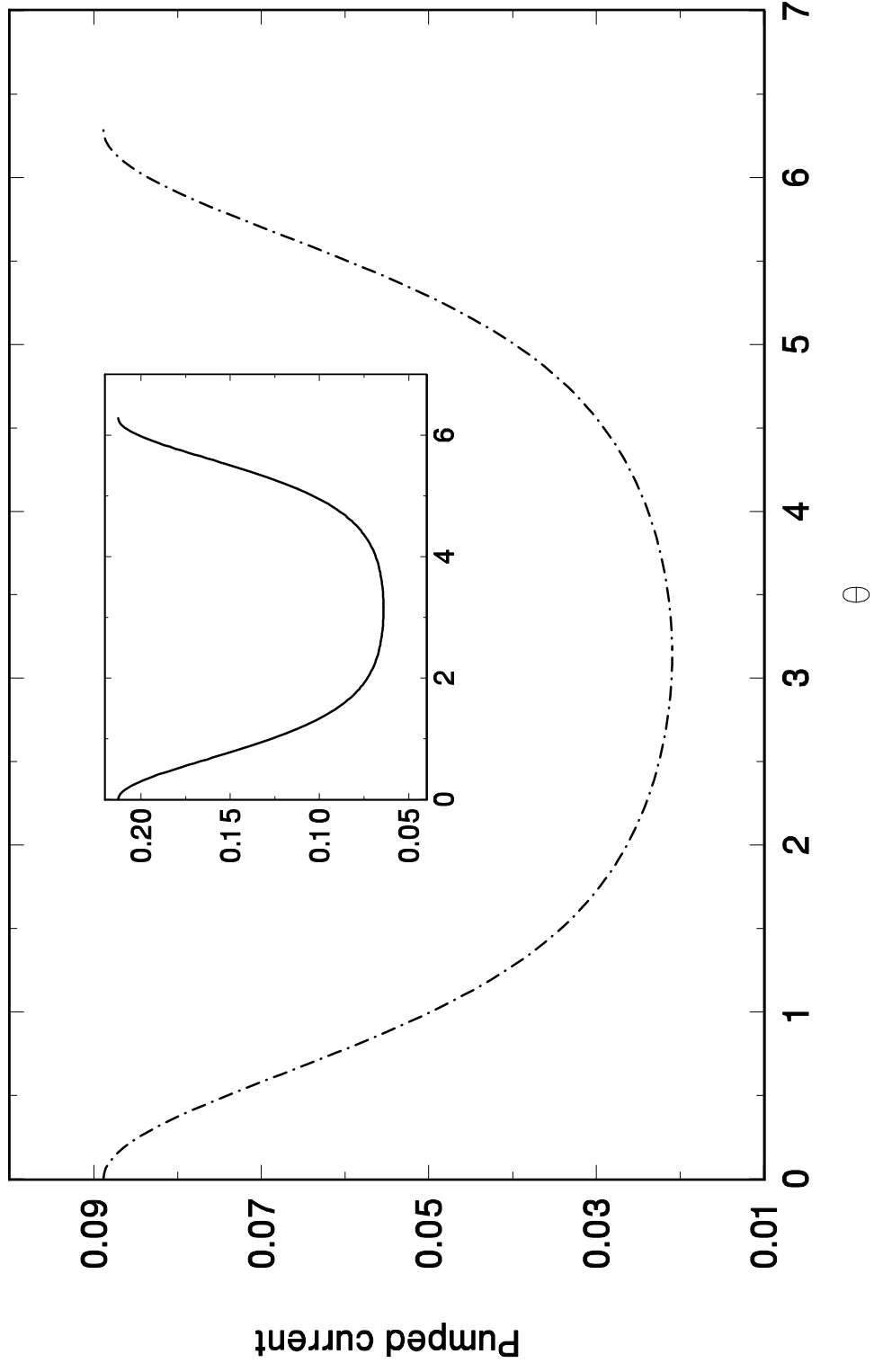


Fig4

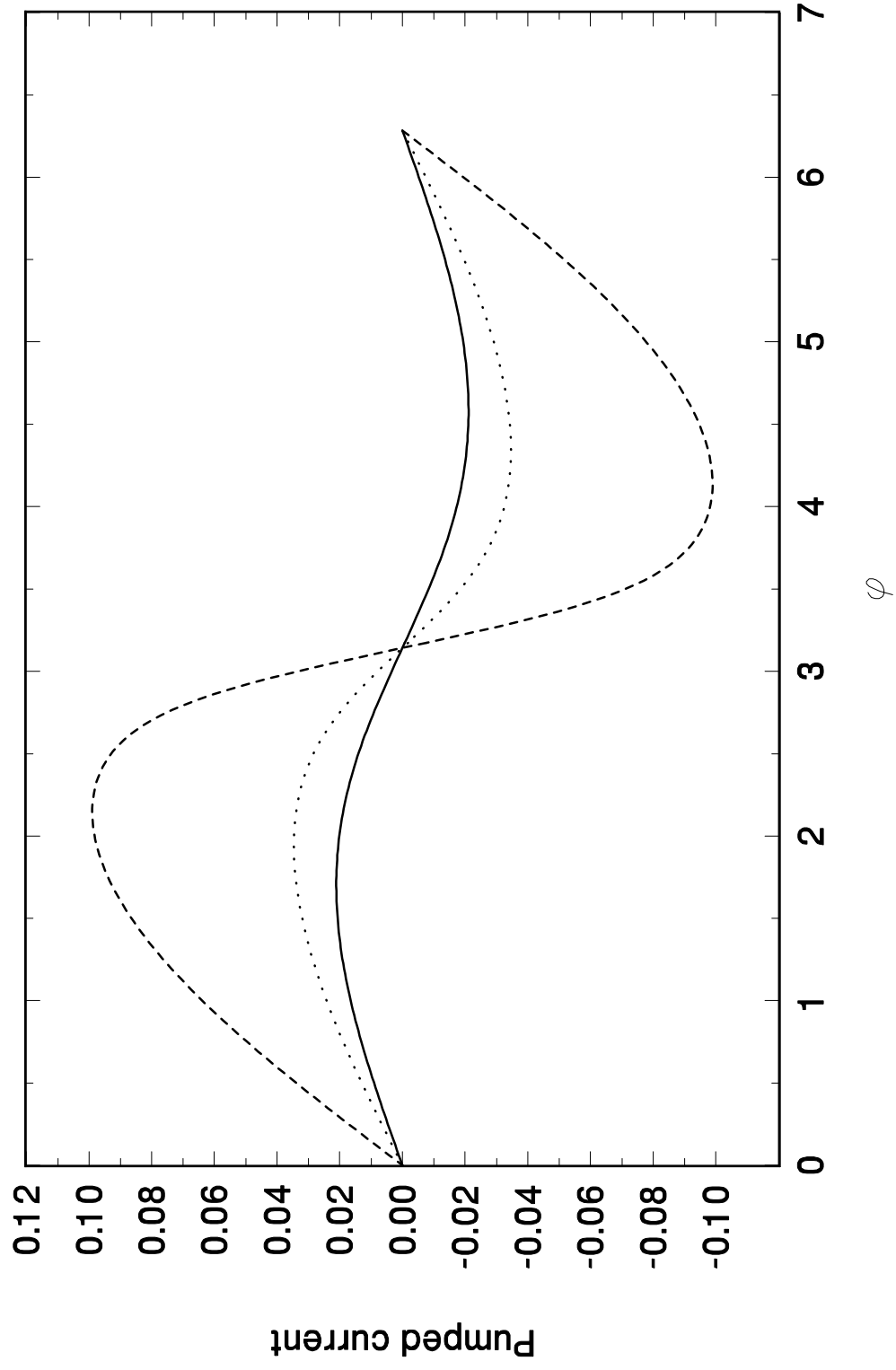


Fig5

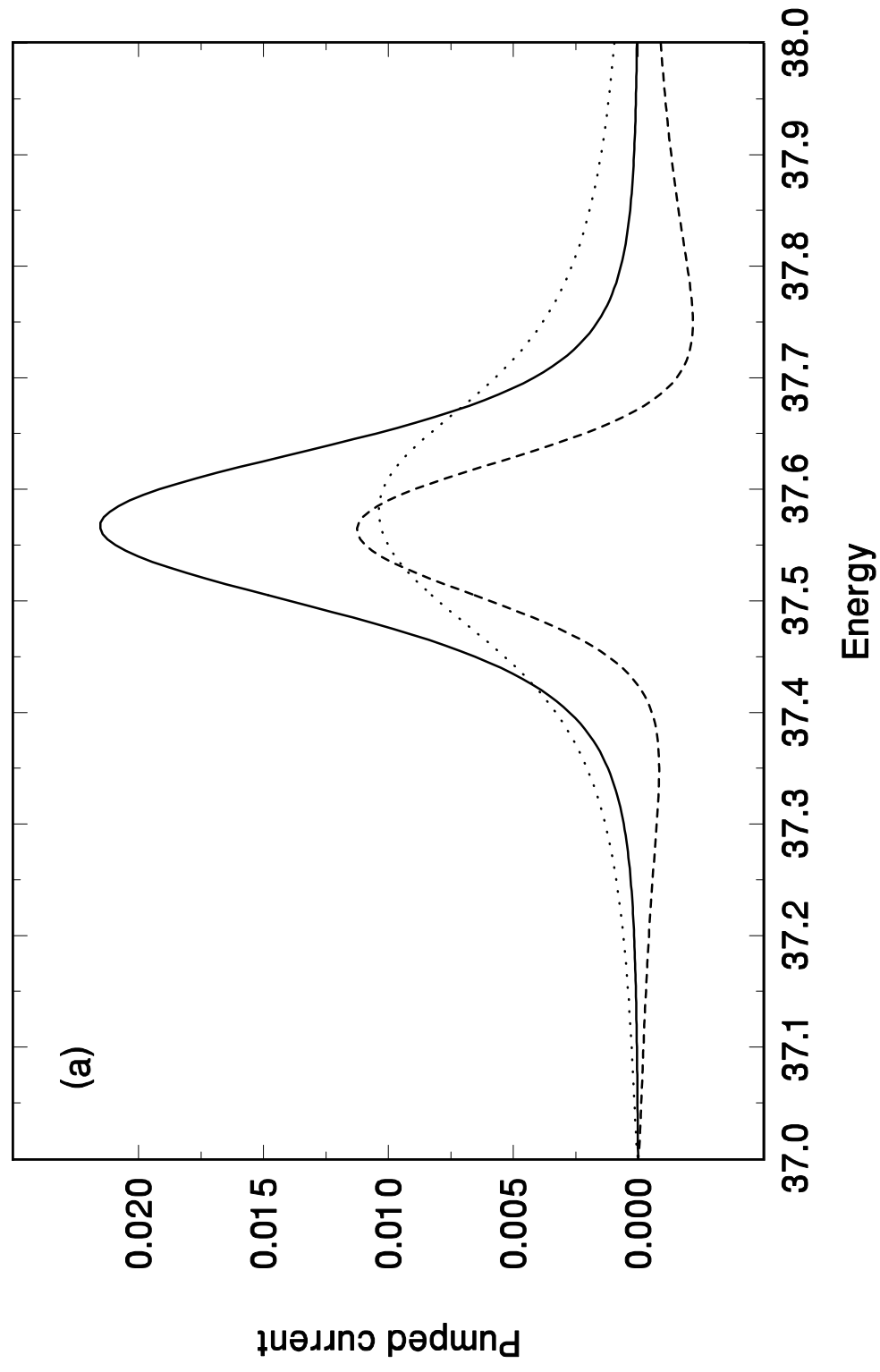


Fig5

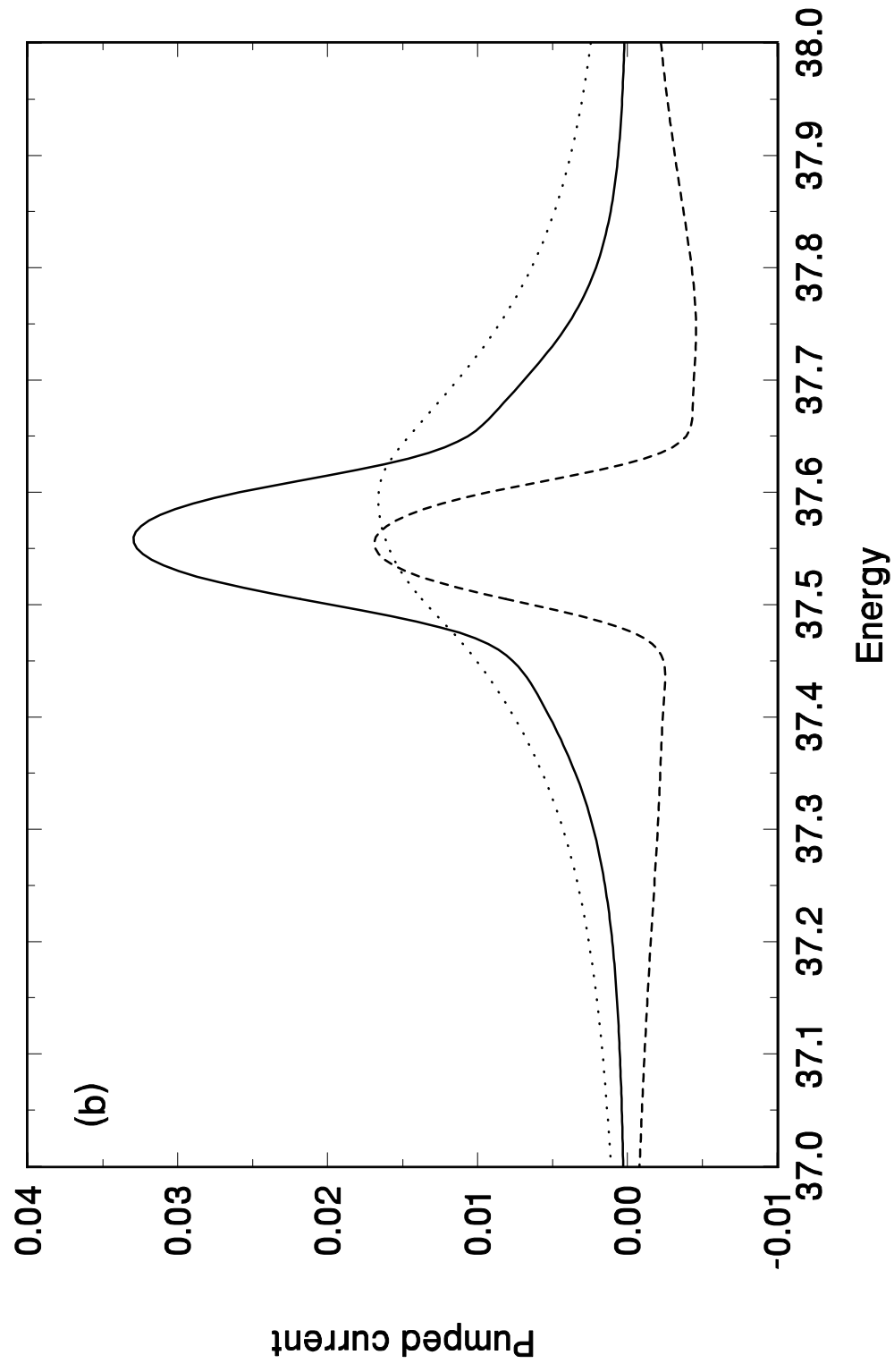


Fig5

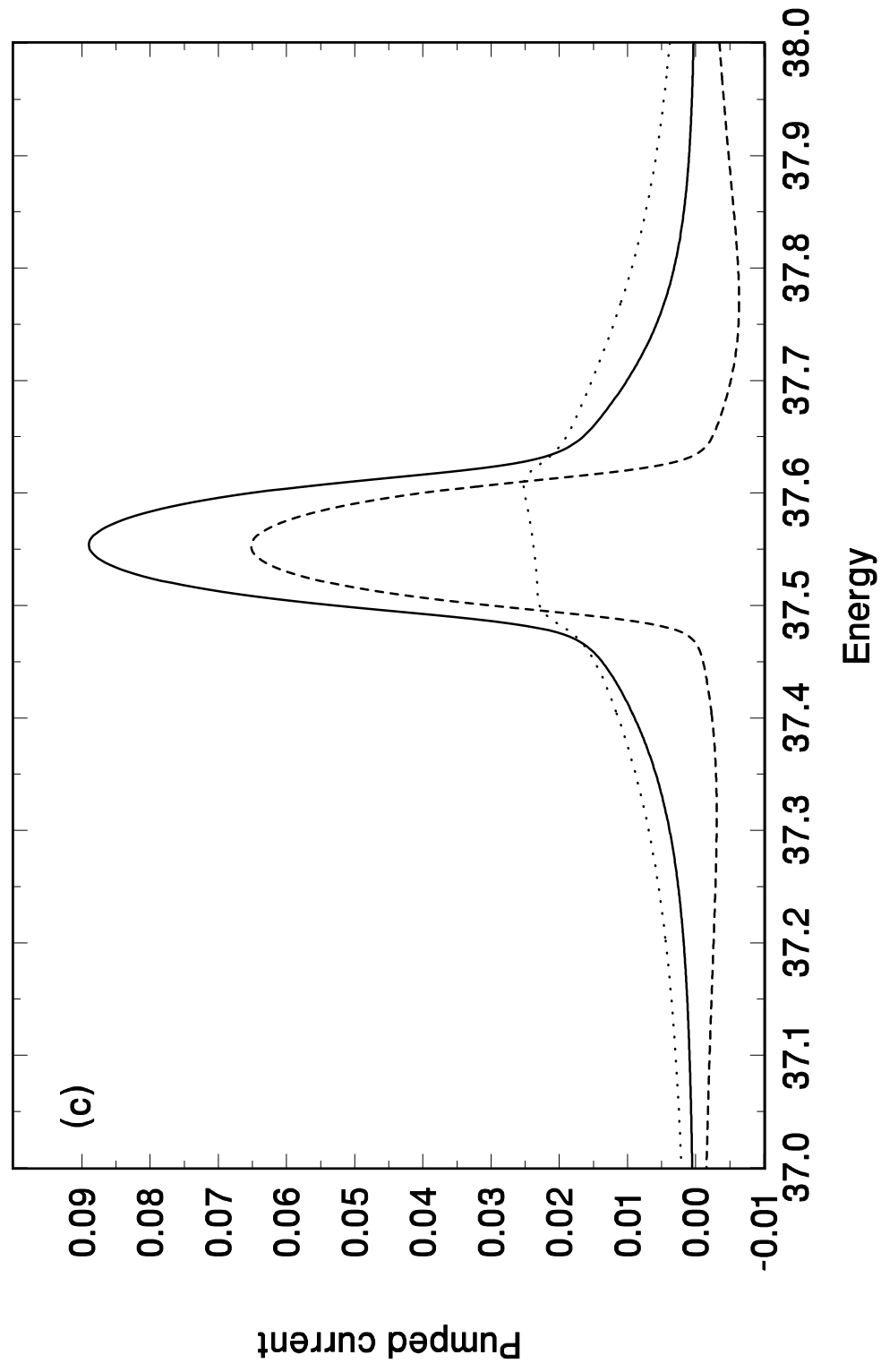


Fig6

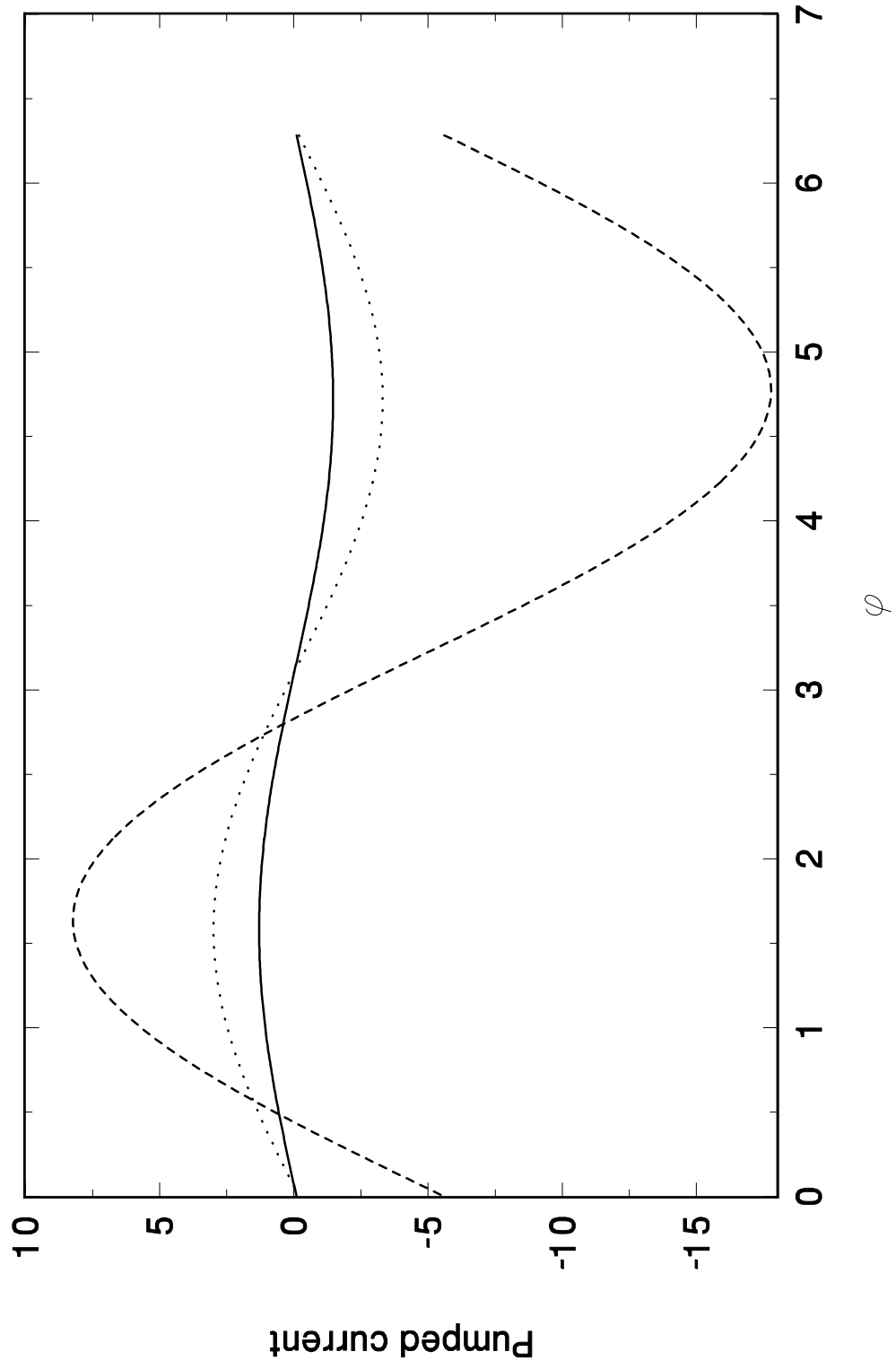


Fig7

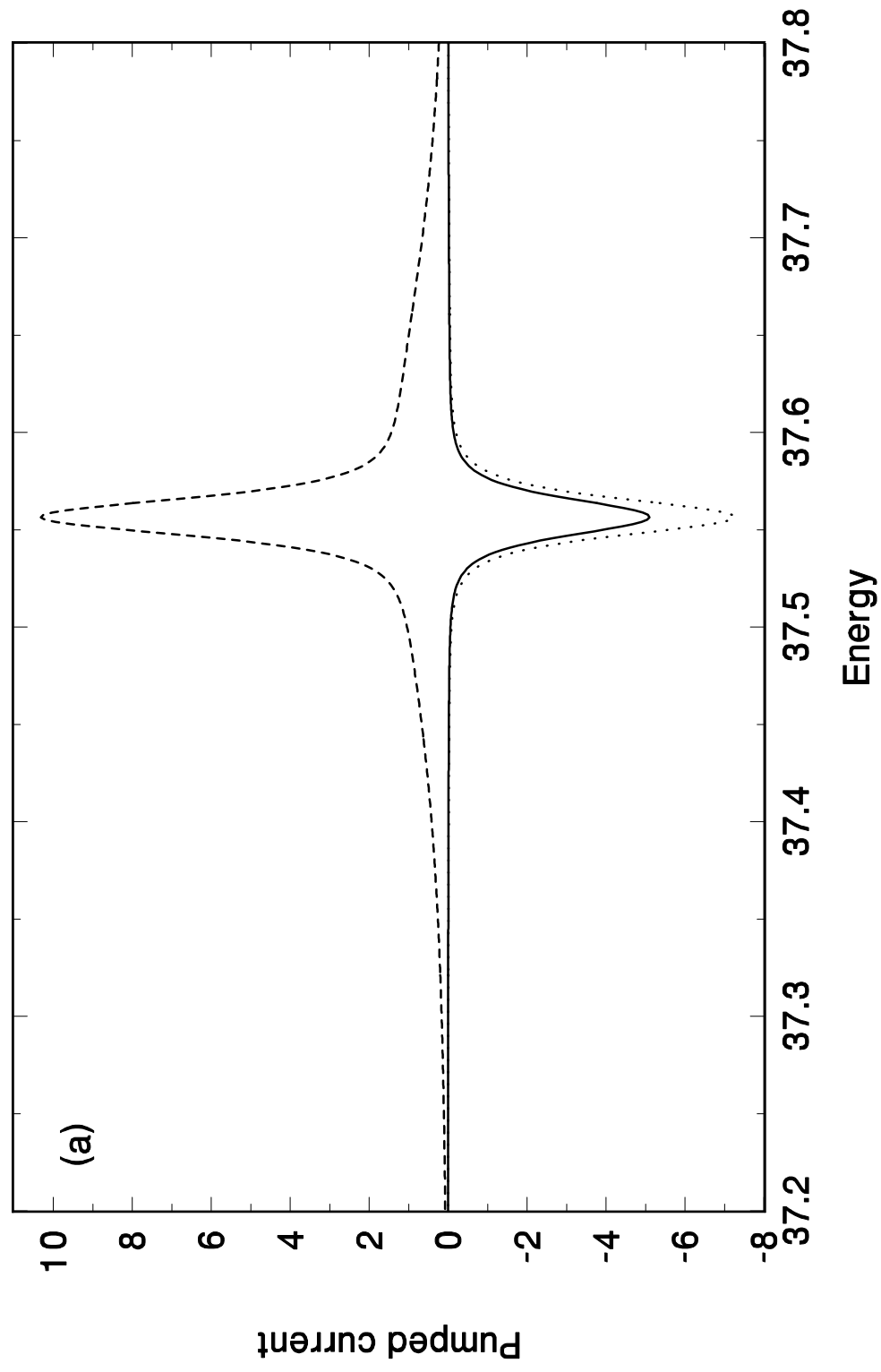


Fig7

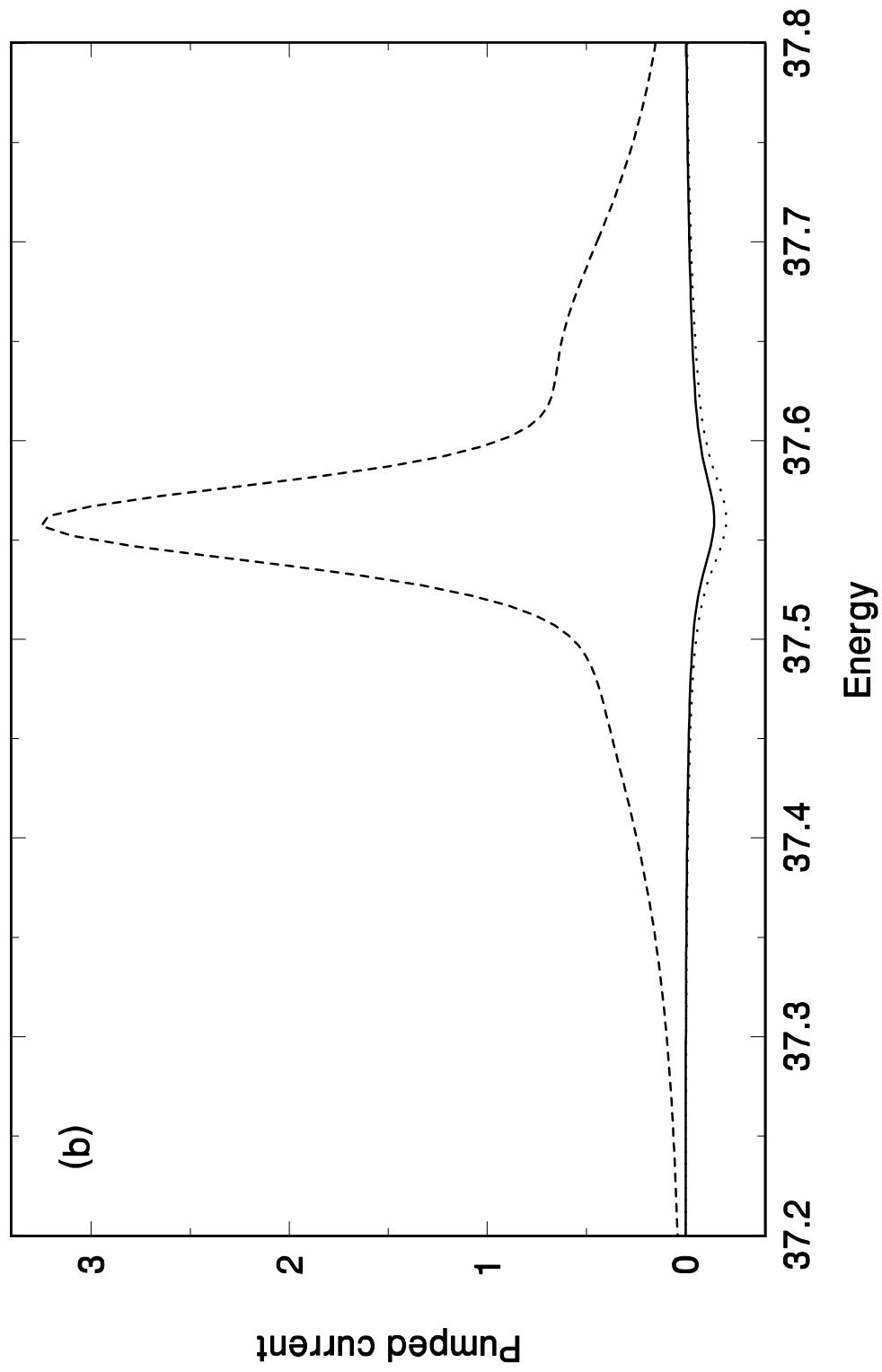


Fig7

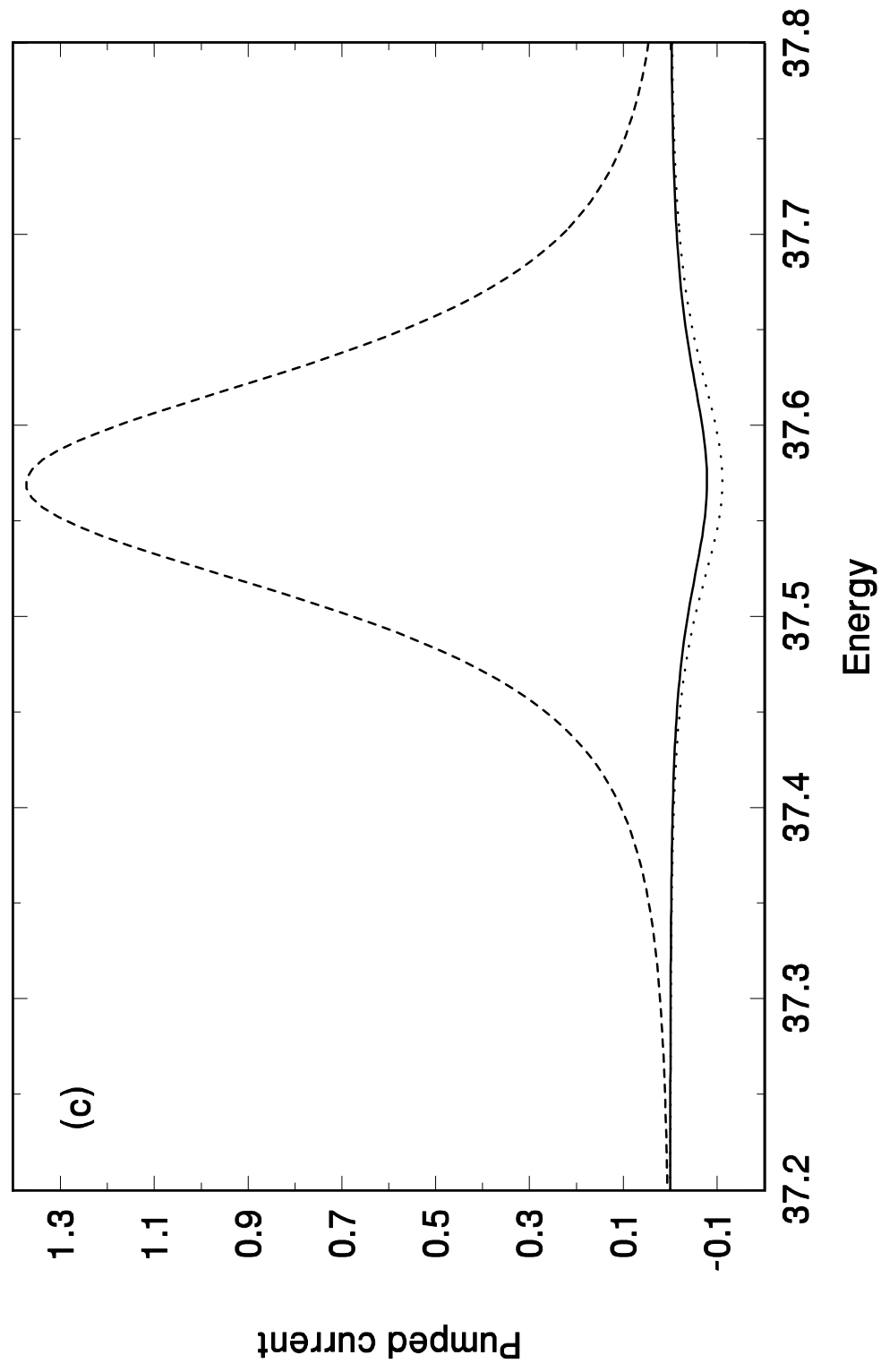


Fig8

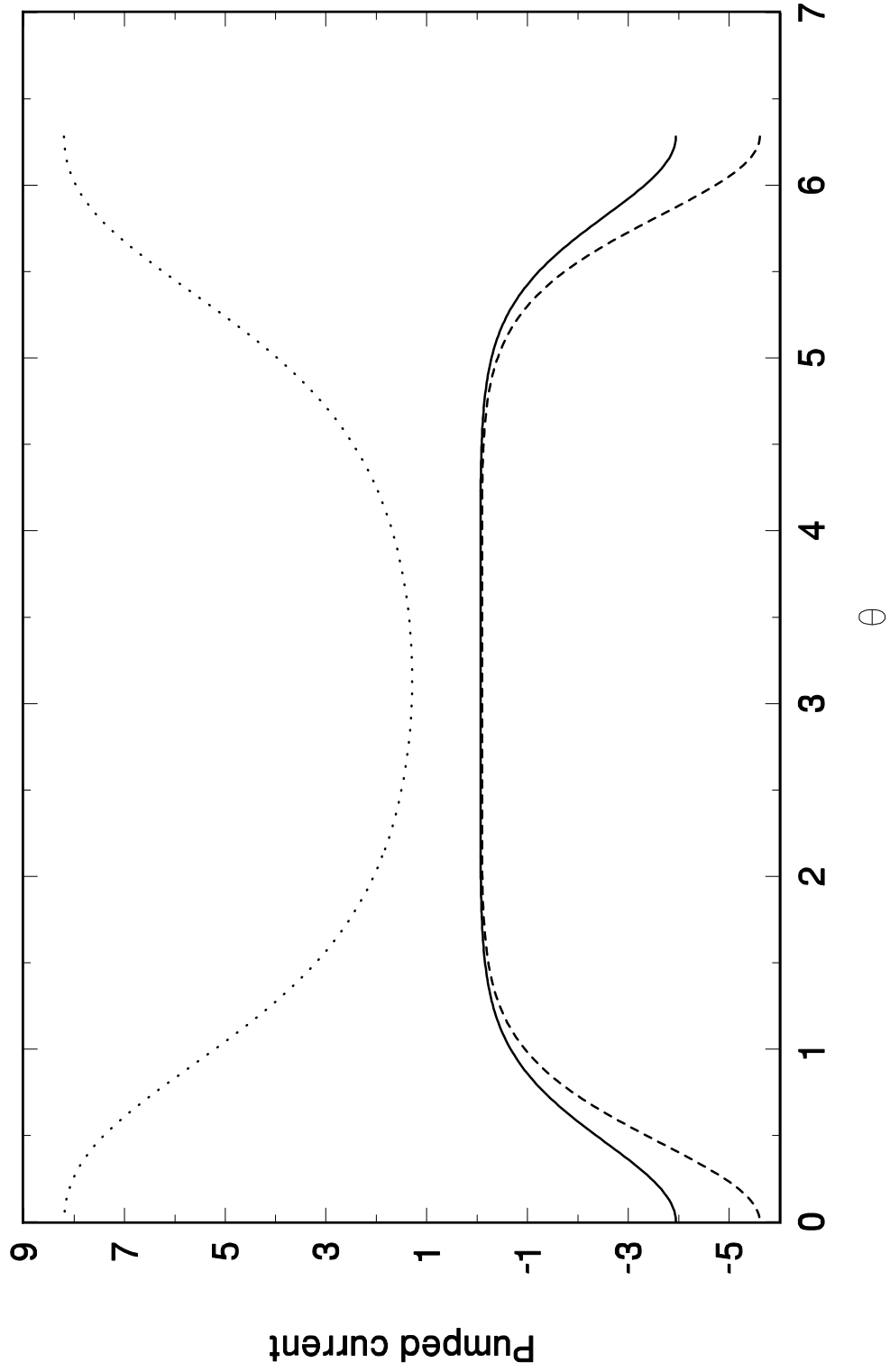


Fig9

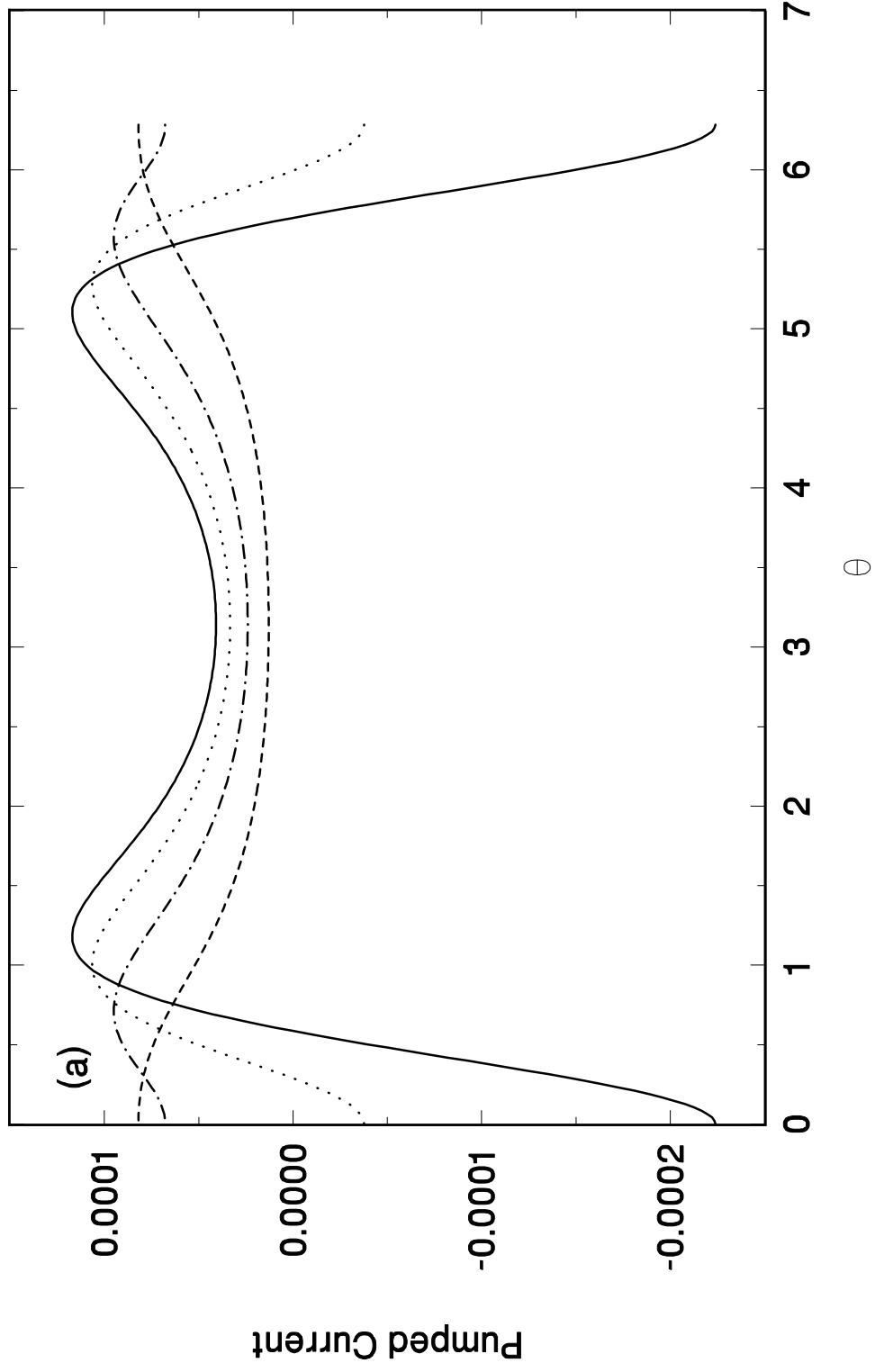


Fig9

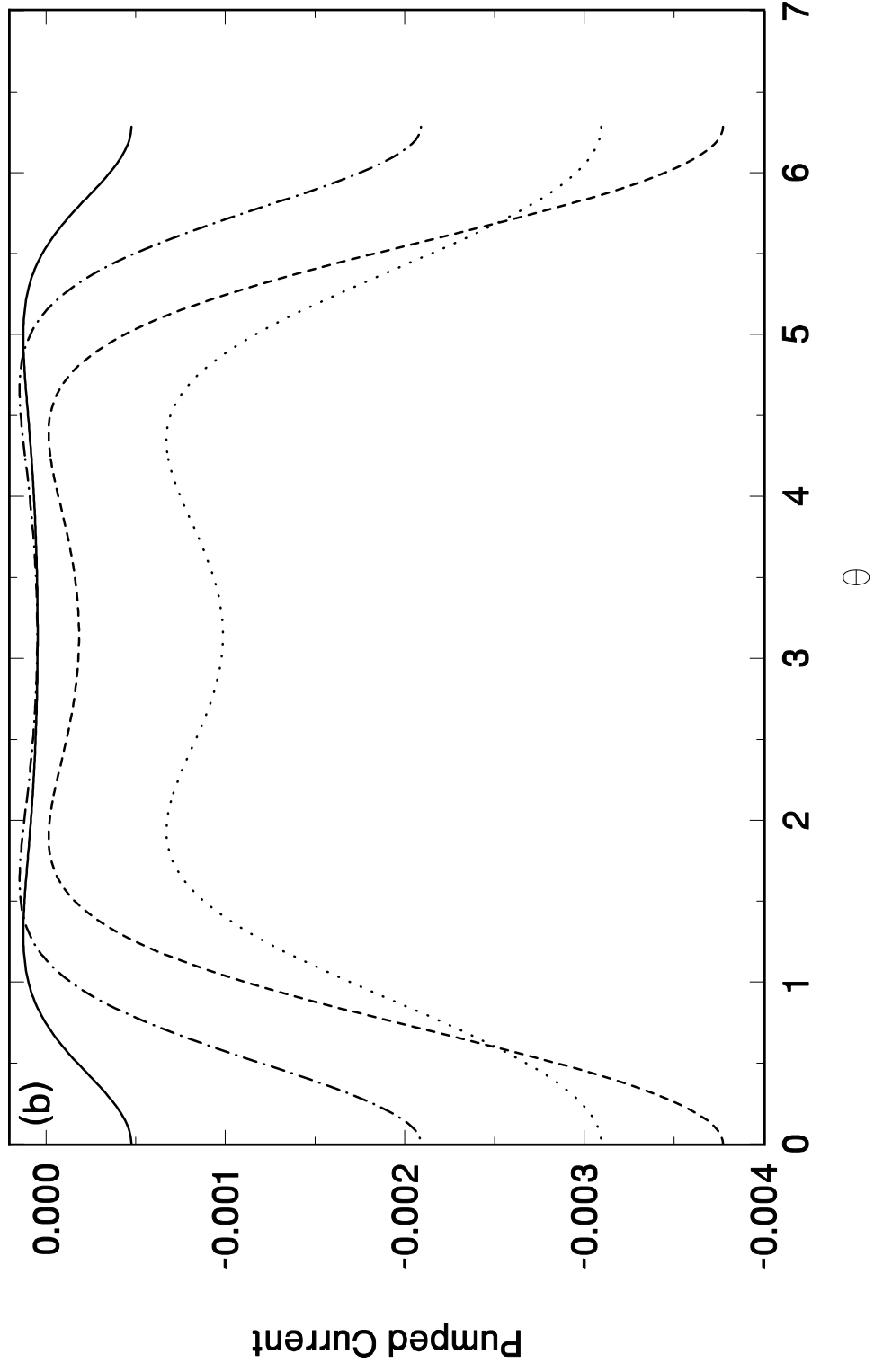


Fig1 0

